2024
11(3), 671

Chemical Biology
LETTERS

Acetamiprid exposure causes molecular and structural changes in the liver and kidney tissues of rats

Annu Phogat, Jagjeet Singh, Reena Sheoran, Arun Hasanpuri, Vinay Malik

Department of Zoology, Maharshi Dayanand University, Rohtak-124001, Haryana, India

Submitted on: 03-Apr-2024, Accepted and Published on: 24-May-2024

Article

ABSTRACT

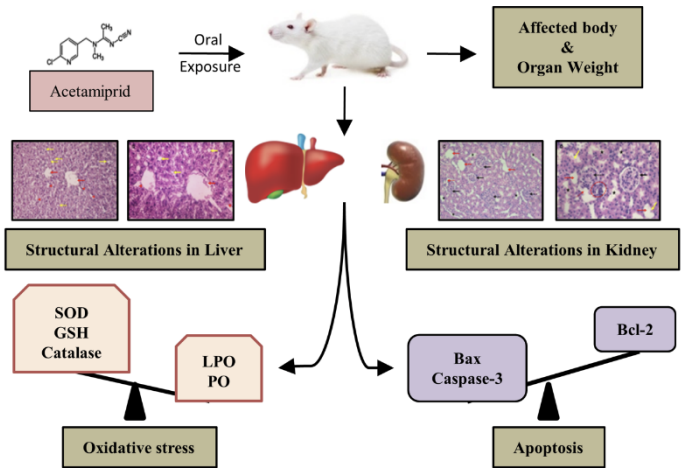

The toxic effects of acetamiprid (ACMP) insecticide in the liver and kidney tissues of rat have been investigated by administering rats intragastrically with 21.7 mg/kg b.wt; 1/10th LD_{50} of ACMP for 21 days. The oxidative stress was confirmed by the increased oxidative injuries to the lipids and proteins, depleted activity of superoxide dismutase and catalase enzymes in both the liver and kidney tissue of rats. Similarly the Glutathione levels were also depleted significantly as compared to control rats. The RT-PCR analysis revealed that exposure to ACMP significantly upregulated the mRNA expression of pro-apoptotic markers (Bax & caspase-3) in both liver and kidney tissue of rats. Furthermore, the exposure of ACMP altered the histo-architecture of both organs where broadening of sinusoidal space, dilated central vein, and vacuolization in the liver tissues while appearance of the cortical cyst, loss of bowman's space, distortion of capillary tuft, and hypertrophied glomerulus in the kidney tissues was detected. Altogether this toxicology study confirms the adverse effects of ACMP and emphasizes the need for strict regulation and more mechanistic understanding to delineate the toxicity of ACMP in mammals.

Keywords: Acetamiprid, Apoptosis, Toxicity, Histopathology, Oxidative stress

INTRODUCTION

Pesticides are synthetic chemicals, deliberately used to control crop pests. The pesticides improve the food quantity for living beings but also lead to severe environmental and health issues.[1] Persistence and extensive use of these xenobiotics have led to their percolation into water sources, and contamination of food chains; causing exposures to wildlife and humans.[2,3] The exact numbers for indirect exposure are far beyond the evaluation, as humans and animals consume contaminated vegetables, fruits, water, and crops. However, direct exposure is primarily reported in pesticide manufacturing units and farm workers.[4,5] As per estimation by the World Health Organisation, nearly 3 million people suffer due to direct pesticide exposures, of which nearly 18000 succumb to death every year in developing countries emphasizing the problem of pesticide poisoning.[6]

Acetamiprid (ACMP) is a systemic chlorinated neonicotinoid pesticide. It is widely used against aphids, leafhoppers, and flies damaging leafy vegetables, grapes, tomatoes, cotton, potatoes, and ornamental plants.[7] ACMP and its residues have been detected in soil, water sources, and food grains.[8] Metabolites of ACMP have also been reported from blood, urine, and different body tissues of humans with known as well as unknown sources of ACMP contamination.[9–12] In humans, its exposure causes headache, vertigo, sleep disorders, vomiting, convulsion, and tachycardia.[13] Several recent studies have reported hepatotoxicity, neurotoxicity, nephrotoxicity, reproductive toxicity, and haematological toxicity of ACMP in various organisms.

A plethora of evidence has indicated oxidative stress as the main driving force behind ACMP-induced organ toxicity. Oxidative stress generation is known to alter cellular biochemistry by damaging biomolecules and altering several enzymes. Recent studies have documented a significant increase in lipid peroxidation, protein oxidation, and functional alterations in protein and lipid chains in liver tissue under oxidative stress.[14,15] Depletion of endogenous antioxidative enzymes like catalase, superoxide dismutase (SOD) along with glutathione (GSH) is speculated as evidence of oxidative stress. These

*Corresponding Author: (Vinay Malik, Department of Zoology, Maharshi Dayanand University, Rohtak 124001, India)
Email:vinaymalikzoo@mdurohtak.ac.in

URN:NBN:sciencein.cbl.2024.v11.671

https://pubs.thesciencein.org/cbl

antioxidative enzymes are the first line of defence against reactive oxygen species. Depletion of these antioxidants allows oxidative stress that causes severe changes inside tissues including the initiation of apoptosis. Apoptosis is a complex chemical cascade and can be speculated as a birth child of oxidative stress. Some recent studies have documented apoptosis in the liver and kidney tissues of rats following pesticide exposure-induced oxidative stress.[16–18]

The liver and kidney are the prime organs involved in metabolism and excretion. Previous studies have reported lipid peroxidation, protein oxidation, antioxidative deficits, and structural changes following xenobiotic exposures in mammals.[19–21] Although some studies have investigated the toxicity of ACMP in the liver or kidney; the literature is almost silent about oxidative stress and its associated toxic effects on apoptotic and structural changes in both kidney and liver tissue of rats. Thus the current study was aimed to provide mechanistic insight into biochemical and molecular changes associated with ACMP toxicity.

MATERIALS AND METHODS

2.1 Chemicals

Acetamiprid (Cat No-33674), ethylenediamine tetraacetic acetic acid (EDTA), thio-barbituric acid (TBA), guanidine, nitroblue tetrazolium (NBT), 5,5'-dithio-bis-(2-nitrobenzoic acid) (DTNB), trichloroacetic acid (TCA), sucrose, and hydroxylamine hydrochloride were purchase from Sigma Aldrich, St Louis, USA. Triton-X-100 and dinitrophenylhydrazine (DNPH) were from Sisco Research Laboratory, Mumbai, India. dNTP mix and Taq polymerase were obtained from Fisher Scientific, Mumbai, India. Primary and secondary antibodies were purchased from Santa Cruz Biotechnology, California, USA.

All other chemicals were of analytical grade with the highest purity. The glassware and plastic ware were sterilized before use.

2.2 Animals and their care

Male Wistar rats (*Rattus norvegicus*) weighing 160 ± 15 g were kept in well-ventilated rooms (temperature of 24 ± 2°C, relative humidity 50 ± 10%) and 12 h alternate light and dark cycle. Rats were fed with a standard pellet diet and water *ad libitum*.

2.3 Experimental design

The experimental rats were randomly divided into two groups containing six animals in each group. Control group rats received 0.5 mL of normal saline (vehicle), intragastrically for 21 consecutive days. Acetamiprid-exposed group rats received 0.5 mL of ACMP (21.7 mg/kg b.wt) dissolved in water intragastrically for 21 consecutive days. The selected dose of ACMP is 1/10th of the reported LD_{50} of ACMP in rats i.e. 217 mg/kg b.wt. The same dose has been used by various earlier studies showing the toxic effects of ACMP.[22,23]

Rats were fasted overnight to bring the metabolic rate to base levels. After 24 h of the last treatment, rats were anaesthetized under CO_2 asphyxiation and sacrificed. Liver and kidney tissue were excised, washed with ice-cold saline, and immediately used for biochemical assays and processed for PCR and western blotting, while a portion of tissues was fixed in 10% formalin solution for histopathological examination.

2.4 Preparation of tissue homogenate

0.5 g of liver and kidney tissue was homogenized in 5 mL of homogenizing medium (pH 7.4) containing 0.25 M sucrose, 1 mM EDTA and 5 mM tris; using a glass dounce tissue homogenizer (Perfit, Ambala, India). Cellular debris was removed after centrifuging homogenate in refrigerated centrifuged (Velocity 18R, Dynamica, Hong Kong) at 2100×g at 4°C for 15 min, and the supernatant was again centrifuged at 13000×g for 2 min. The obtained supernatant was used for biochemical assays.

2.5 Body and organ weight assessment

The body weights of all animals were measured each week while weights of tissues were measured once after the dissection of all experimental animals.

2.6 Analysis of lipid peroxidation and protein oxidation

Lipid peroxidation was assayed in rat liver and kidney homogenate as described previously.[24] Oxidative damage to membranous lipids was measured by estimating malondialdehyde (MDA) content using a spectrophotometer (Shimadzu UV-2450, Kyoto, Japan). The results were expressed as nmol MDA/mg protein.

Protein oxidation was determined spectrophotometrically at 370 nm by measuring the hydrazones formed by the reaction of DNPH with protein carbonyl present in the tissue.[25] The protein carbonyl content was expressed as nmol carbonyls/ mg protein.

2.7 Analysis of antioxidant defence biomarkers

Catalase activity was assessed by estimating the decomposition rate of H_2O_2 to water and oxygen according to methods described previously.[26] The change in absorbance was read spectrophotometrically at 240 nm and results were expressed as µmol of H_2O_2 oxidized/min/mg protein.

Superoxide dismutase activity was assayed in liver homogenate as described previously.[27] The rate of inhibition of NBT reduction by hydroxylamine hydrochloride produced free radicals was measured spectrophotometrically at 560 nm. The enzyme quantity needed for 50% inhibition was determined and the results were expressed as U/mg protein.

Glutathione content was estimated as described earlier [24]. The process involves thiol-mediated reduction of DTNB to 2-nitro-5-mercaptobenzoic acid producing intense yellow colour. The colour change was read at 412 nm, and the results were expressed as nmol GSH/mg protein.

2.8 Molecular docking analysis

The crystallographic 3-dimensional structures of Bax and Bcl-2 proteins with PDB IDs (5W62 and 1G5M) were retrieved from RCSB-PDB. The proteins were prepared for docking by the Energy Minimisation process performed using UCSF Chimera software, the retrieved PDB structures were subjected to the deletion of non-standard amino acids & chains, the deletion of H_2O molecules, and the addition of Hydrogen molecules.

Blind Molecular Docking was performed using PyRx (an open-source software) that works with Autodock Vina 1.1.2. The energy-minimized PDB structures from UCSF Chimera were loaded into the virtual screening software interface PyRx. The

grid box's size and coordinates were adjusted by tracking the boundary lines of the grid around the active binding site or by giving the appropriate coordinate values & docking was performed. The 2D and 3D Molecular interactions between ligand & receptor molecules were analysed using Discovery Studio Visualizer.

2.9 Apoptotic gene expression analysis

Total RNA was isolated using an RNA extraction kit (NP-84105, Nucleopore) according to the manufacturer's instructions. Concentration and purity (A260/280) of RNA were determined using a Nanodrop spectrophotometer (DS-11 FX+, Denovix, USA). Total RNA (2.5 µg) from each sample was reversely transcribed to cDNA using the RevertAid First-strand synthesis kit, following the manufacturer's instructions. Semi-quantitative PCR was performed on a gradient thermal cycler (PeqStar 2X, PEQLAB, Erlangen, Germany) using 1 µL cDNA.

Specific primers for Bax, Bcl-2, caspase-3, and β-actin were designed using Primer 3 software (Table 1). Initial denaturation was done at 94°C (2 min) following 30 cycles of amplification consisting of denaturation (94°C, 30 sec), annealing (30 sec), and extension (72°C, 1 min). The PCR products were subjected to agarose gel electrophoresis (1.8% w/v) and bands were visualized and photographed using the gel documentation system (Biorad Laboratories, California, USA). The intensity of bands was quantified with Image J software using β-actin as standard.

Table 1. Sequence of specific primers used for semi-quantitative PCR analysis.

Primer (Accession)	Primer sequence (5'-3')	Size (bp)
Bax (NM_017059.2)	F- GGCTGGACACTGGACTTC R- CAGATGGTGAGTGAGGCA	152
Bcl-2 (NM_016993.2)	F- GTGGACAACATCGCTCTG R- AGACAGCCAGGAGAAATCA	141
Caspase-3 (NM_012922.2)	F- GACAACAACGAAACCTCC R- AGGGTAATCCTTTTGTAACTG	122
β-actin (V01217.1)	F- TTGCCCTAGACTTCGAGCAA R- AGACTTACAGTGTGGCCTCC	213

2.10 Western Blot Analysis

Liver and kidney tissues were homogenized with lysis buffer (30 mM Tris-HCl, pH 7.4, containing 10mM EGTA, 5mM EDTA, 1% Triton X-100, 250 mM sucrose, and protease inhibitor) and centrifuged at 2100 × g for 10 min and the supernatant was collected and centrifuged at 13000 × g for 15 min to obtain mitochondrial and cytosolic fraction for cytochrome c protein expression analysis. 20 µL sample containing 80 µg protein was subjected to 12% SDS-PAGE followed by blotting on the nitrocellulose membrane. The nitrocellulose membrane was blocked with 5% skim milk protein in phosphate buffer saline (PBS) for 2 h at room temperature, followed by incubation with primary antibody of cytochrome c with 1:400 dilutions for 4 h. After this, the membrane was washed twice with PBS and once with PBS containing tween-20 for 10 minutes. The membrane was incubated with corresponding secondary antibodies with 1:10000 dilutions for 1 h at room temperature. After washing twice with PBS for 10 minutes each, immunoreactive cytochrome c protein was visualized by TMB and analyzed using Image J software.

2.11 Histopathological examination

After fixation in 10% formalin for 24 h, tissues were washed properly, dehydrated using a gradual series of ethyl alcohol, and embedded in paraffin. Tissue sections (5 µm thicknesses) were cut using the microtome (MRM-AT, Medimeas, Ambala, India), deparaffinized, stained with Hematoxylin and Eosin, and mounted with DPx. Slides were examined under a light microscope equipped with a digital camera (Nikon Eclipse Ci-L, Tokyo, Japan).

2.12 Protein determination

The protein content was determined following Lowry's method using BSA, as a standard protein.[28]

2.13 Statistical analysis

The results were expressed as mean ± SD. Results were statistically analyzed using the Students' *t*-test. A p-value ≤0.05 was considered statistically significant.

RESULTS

3.1 Effects on body and organ weight

Body weight and organ weight results are summarised in Table 2. Exposure to ACMP had significant (p≤0.01) detrimental effects on final body weight and reduced the gain of body weight significantly (p≤0.01). The relative liver weight of ACMP-exposed rats differed significantly (p≤0.05) from control rats. On the other hand, no significant changes were observed in the relative kidney weight of control and ACMP-exposed rats.

Table 2. Effect of acetamiprid on weight parameters in rats.

	Initial Body Weight (g)	**Final Body Weight** (g)	**Weight Gain** (g)	**Relative organ weight (%)**
Liver				
Control	139 ± 4.9	189.8 ± 10.8	50.8 ± 7.5	3.97 ± 0.2
ACMP-exposed	136.4 ± 6.1	169.2 ± 5.8**	32.8 ± 5.1**	3.52 ± 0.4*
Kidney				
Control	139 ± 4.9	189.8 ± 10.8	50.8 ± 7.5	0.61 ± 0.0
ACMP-exposed	136.4 ± 6.1	169.2 ± 5.8**	32.8 ± 5.1**	0.60 ± 0.0

Values are presented as Mean ± S.D. (n=5). * is p≤0.05; ** is p≤0.01. ACMP -acetamiprid.

3.2 Effects on lipid peroxidation and protein oxidation

The results of lipid peroxidation and protein oxidation are represented in Figure 1. Compared to control rats, exposure to ACMP significantly elevated the peroxidation of lipids and oxidation of proteins in liver tissue. Similarly, exposure to ACMP significantly caused an increase in lipid peroxidation and protein oxidation compared to control rats in kidney tissue of rats.

3.3 Effects on antioxidant defence system

Exposure to ACMP significantly depleted the activity of superoxide dismutase and catalase enzymes in both the liver and kidney tissue of rats as compared to control rats. Glutathione levels were also depleted significantly in both liver and kidney

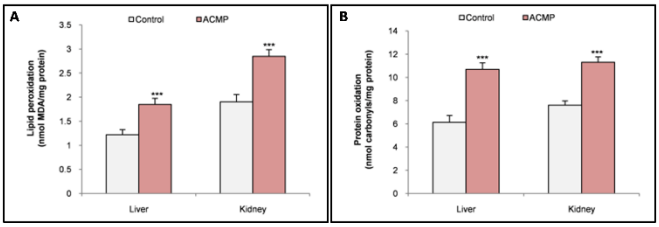

Figure 1. Exposure to ACMP caused oxidative injuries to lipids and proteins: **A-** Lipid peroxidation; **B-** Protein oxidation. Values are presented as Mean ± S.D. (n=5). *** is p≤0.001. ACMP - acetamiprid.

tissues following ACMP exposure (Table 3).

3.4 Molecular docking interpretation

Molecular docking of Bax protein with acetamiprid showed a binding energy of -4.47 ± 0.12 and was found to form 5 interactions with PRO 13, GLN 18, LEU 59, GLU 159 and LEU 162 residues. While, results of molecular docking of Bcl-2 protein with acetamiprid revealed a higher binding energy of -5.18 ± 0.38 and was found to form 11 interactions with THR 7, TYR 9, GLY 8, ASP 10, ASN 11, HIS 186, ILE 189, GLN 190, GLY 194, TRP 195and ASP 196 residues (Figure 2) (Table 4).

Table 3. Effect of acetamiprid on endogenous antioxidants in liver and kidney tissue of rats.

	SOD activity (U/mg protein)	Catalase activity (µmol H_2O_2 oxidized/ min/mg protein)	GSH content (nmol GSH/mg protein)
Liver			
Control	56.32 ± 5.57	48.44 ± 5.09	91.64 ± 6.69
ACMP-exposed	34.81 ± 4.38***	30.15 ± 3.01***	65.37 ± 4.90***
Kidney			
Control	40.08 ± 4.88	38.77 ± 3.77	58.94 ± 5.70
ACMP-exposed	25.01 ± 2.33***	25.19 ± 2.84***	39.29 ± 4.93***

Values are presented as Mean ± S.D. (n=5). *** is p≤0.001. ACMP - acetamiprid

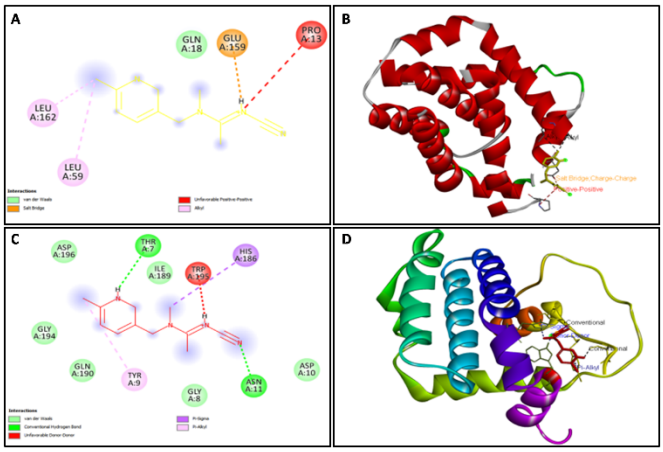

Figure 2. Molecular interaction of apoptotic proteins with acetamiprid: **A, B-** Bax protein, **C, D-** Bcl-2 protein.

Table 4. Details of binding energies and possible binding sites obtained after molecular docking of acetamiprid with ligands.

Protein with PDB id	Binding Energy	Binding sites
Bax (5w62)	-4.467 ± 0.122	PRO (13), GLN (18), LEU (59), GLU (159), LEU (162)
Bcl-2 (Ig5m)	-5.178 ± 0.377	THR (7), TYR (9), GLY (8), ASP (10), ASN (11), HIS (186), ILE (189), GLN (190), GLY (194), TRP (195), ASP (196)

3.5 Effects on apoptotic markers

The effect of ACMP exposure on apoptotic markers was evaluated by reverse transcription polymerase chain reaction (RT-PCR). RT-PCR analysis revealed that exposure to ACMP significantly upregulated the mRNA expression of pro-apoptotic markers (Bax & caspase-3) in both liver and kidney tissue of rats. In contrast, exposure to ACMP significantly downregulated the mRNA expression of anti-apoptotic marker (Bcl-2) in rat's liver and kidney tissues (Figure 3).

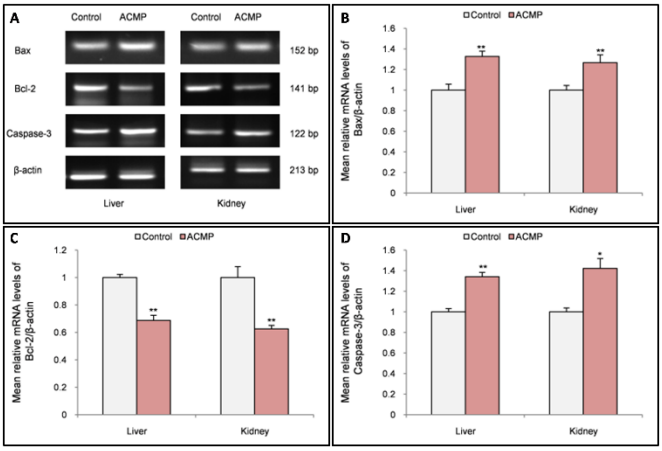

Figure 3. Effects of acetamiprid exposure on apoptotic markers in the liver and kidney tissues of rats: **A-** mRNA expression, **B-** Bax, **C-** Bcl-2, **D-** caspase-3. Results are expressed as Mean ± S.D. (n=3). ACMP-acetamiprid. * is p≤0.05 and ** is p≤0.01.

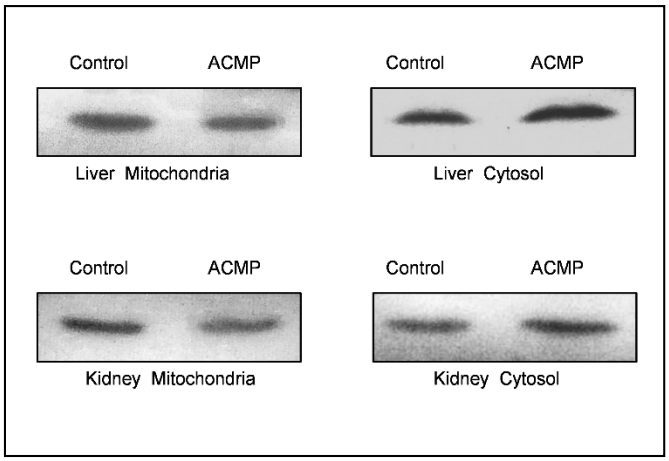

Figure 4. Effects of acetamiprid exposure on localization of cytochrome c protein in cytosol and mitochondria of liver and kidney of rats. ACMP-acetamiprid.

Localization of cytochrome c was evaluated via western blotting. Western blotting results revealed that exposure to ACMP caused the translocation of cytochrome c into the cytosol from mitochondria. While in control rats, cytochrome c remained localised within the mitochondria (Figure 4).

3.6 Effects on histo-architecture of liver and kidney tissues

Histological evaluation was performed with a light microscope to gain insight into the effects of ACMP exposure on the histo-architecture of the liver and kidney tissues of rats. In liver tissue, severe structural alteration i.e. broadening of sinusoidal space, dilated central vein, and vacuolization were noticed after ACMP exposure. While liver tissue of control rats depicted a normal shape of the central vein and hepatocytes along with normal sinusoidal spacing and no signs of vacuolization (Figure 5).

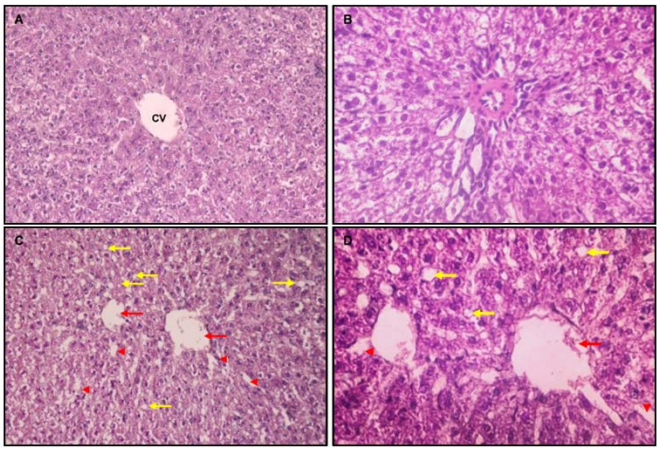

Figure 5. Photomicrograph of liver sections (H & E staining): Control rats **A-** 20X, **B-** 40X, depicting normal shape and arrangements of hepatocytes, sinusoidal spaces, and central vein (CV). Acetamiprid-exposed rats **C-** 20X, **D-** 40X, depicting dilation of central vein (red arrow), broadening of sinusoidal spaces (red arrowhead), and vacuolization (yellow arrow).

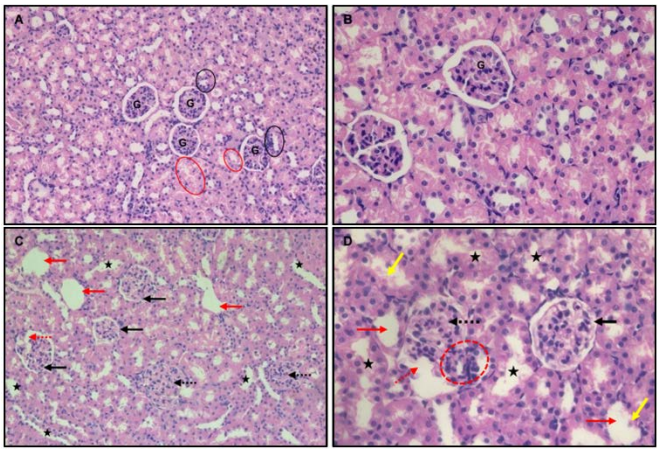

Figure 6. Photomicrograph of kidney sections (H & E staining): Control rats **A-** 20X, **B-** 40X, depicting normal glomerulus (G), distilled convoluted tubules (black circle), and proximal convoluted tubules (red circle). Acetamiprid-exposed rats **C-** 20X, **D-** 40X, depicting cortical cyst (red arrow), loss of bowman's space (black arrow), destroyed capillary tuft (dotted red arrow), hypertrophied glomerulus (dotted black arrow), cellular infiltration (dotted red circle), apoptotic bodies (yellow arrow) and tubular degeneration (star).

In kidney tissue sections of control rats, normal arrangement of the glomerulus, normal proximal convoluted tubules, and distal convoluted tubules, bowman's space were well depicted with intact basement membrane. While in kidney sections of ACMP-exposed rats; the appearance of the cortical cyst, loss of bowman's space, distortion of capillary tuft, and hypertrophied glomerulus were prominently observed. Tubular degenerations, cellular infiltration, and apoptotic bodies were also evident in the kidney tissue of ACMP-exposed rats (Figure 6).

DISCUSSION

Acetamiprid is the second most widely used neonicotinoid after imidacloprid. This pesticide has peculiar physiological and toxicological properties and is reported to cause mammalian toxicity. Some recent studies have reported the toxic effects of ACMP in various organs.[29,30] However, the information related to ACMP-mediated organ toxicity is limited. So, in the present study, we evaluated weight parameters, oxidative stress markers, apoptotic progression, and histopathological alterations in liver and kidney tissues of rats following ACMP exposure

Weight parameters are considered a bio-indicator for the overall health and physiology of organs inside the body. The results of the current study revealed a significant difference in body weight gain in ACMP-exposed groups as compared to non-exposed groups. There were significant changes in relative liver weight, while no significant changes were observed in the relative weight of the kidney in ACMP-exposed rats, suggesting the liver is a more affected organ than the kidney. Collectively, the changes in weight parameters indicated the onset of hepato-renal toxicity of ACMP in rats. These changes might be due to oxidative damage to the lipids and proteins, and structural changes reported in this study. Earlier a study reported oxidative stress along with a significant reduction in body weight of both male and female rats after 8 weeks of exposure to 22 mg/kg b.wt of ACMP.[31] Additionally, few investigations documented the decrease in body weight in mice following 30 mg/kg b.wt of ACMP for 35 days and 40 mg/kg b.wt of ACMP for 28 days of exposure respectively.[32]

Alteration in body weight parameters indicated organ toxicity and injury. We also investigated the oxidative stress markers in the liver and kidney tissue of rats. Subsequently, the effects of ACMP exposure on lipid peroxidation and protein oxidation along with endogenous antioxidant defence system were assessed. Lipid peroxidation and protein oxidation are plausibly the most widely evaluated processes caused by oxidative stress, thus considered as one of the excellent indicators of oxidative stress in biological tissue. Results of the present study showed marked elevation in oxidative injury to lipids and proteins suggesting the adverse effects of ACMP on the physiology of both liver and kidney tissues. Herein, both the liver and kidney were equally affected. Earlier, some studies have also reported similar detrimental effects of ACMP on lipid and protein profiles in the brain, liver, kidney, and testis of rats.[13,15,29,33,34]

Accumulating evidence from recent studies has supported that oxidative stress also involves the over utilizing endogenous antioxidants, especially SOD and catalase along with the uptake of GSH.[35–37] In the present study, exposure to ACMP caused a significant decrease in the activity of SOD and catalase enzymes in both liver and kidney tissues, suggesting that oxidative stress is the main manifestation of ACMP-mediated hepato-renal toxicity. Additionally, GSH levels were significantly reduced in the hepatic and renal tissue of ACMP-exposed rats. The results of this study are in concordance with earlier studies that have also reported the reduction in endogenous antioxidants following sub-acute,[38] sub-chronic,[39,40] and chronic exposure[23,31] of ACMP in rats.

The oxidative stress also affects the progression of apoptosis. In the present study, PCR results revealed that intoxication of ACMP (21.7 mg/kg b.wt) for 21 days significantly upregulated the mRNA expression of pro-apoptotic markers i.e. Bax and caspases-3. Additionally, the mRNA expression of Bcl-2 - an anti-apoptotic protein was significantly downregulated. The increase in pro-apoptotic markers and the decrease in anti-apoptotic markers mark the progression of apoptosis inside tissues. The molecular docking analysis of acetamiprid with Bax and Bcl-2 protein revealed a strong interaction between them and this could have been responsible for the apoptotic effects of acetamiprid as observed in the findings of this study. Earlier, some *in vivo* and *in vitro* studies have also reported ACMP-mediated progression of the apoptotic cascade by altering Bax, Bcl-2, and caspases-3 levels.[41,42] The release of cytochrome c from mitochondria to cytosol is a bio-indicator and conforming step for apoptosis. The protein expression analysis revealed that exposure to ACMP caused the release of cytochrome c from mitochondria to cytosol in rats' liver and kidney. Apart from the apoptotic cascade induced by increased Bax and caspase-3, another possible reason for the release of cytochrome c is the increased lipid peroxidation that weakened the biomembrane of hepatic and renal tissue. The apoptotic changes reported in the present study correlate with previous studies' findings that have depicted cytochrome c release as a marker step for apoptosis during ACMP exposure[41] and other pesticide toxicity.[43,44]

Histopathological examination revealed the severe structural alteration in liver and kidney tissues of ACMP-exposed rats. These results agree with this study's biochemical findings and apoptotic changes. The increased oxidative injury to cellular biomolecules and apoptosis affects the cellular biochemistry and physiology that might be reflected in structural analysis. Dilation of the central vein, broadening of sinusoidal spaces, and vacuolisation were evident structural alterations in hepatic tissue. Similar structural alterations were observed after ACMP exposure in some previous studies.[14,23] In kidney tissue, the appearance of cortical cysts, narrowing of bowman's space, and tubular degeneration were observed and were in line with the findings of some recent studies concerning exposure to ACMP.[30,33,45] Cellular infiltration, distortion of capillary tuft, and apoptotic bodies are indicators for cellular damages that can be correlated with the apoptotic findings of this study. Additionally, the histopathological findings reported in this study are similar to other studies performed during acute pesticide exposure,[46] sub-chronic exposure[40] and ageings;[47] suggesting these changes as bio-indicators for the hepato-renal toxicity of pesticides and diseased conditions.

Conclusion

In conclusion, the weight parameters, biochemical assessment, apoptotic insight, and histopathological evaluation indicated that ACMP exposure (21.7 mg/kg b.wt, 1/10th LD_{50}) for 21 days has severe toxic effects on hepato-renal tissues of rats. The underlying mechanism of ACMP exposure-mediated toxicity can be associated with oxidative stress, possibly by altering biochemical well-being and eliciting apoptosis. Therefore, more awareness about using and handling ACMP is recommended to avoid direct environmental contaminations. It is also highlighted that more mechanistic scientific investigations should be carried out to delineate the mechanism of ACMP toxicity and to find potential therapeutics for the toxicity.

Acknowledgements

Funding: The authors received no specific funding for this work.
Ethics statement: The study was duly approved by the Institutional Animal Ethics Committee (Reg No. 1767/GO/Re/S/14/CPCSEA) (Approval no. 76-85). All the protocols involving animals were done according to the guidelines of the Committee for the Purpose of Control and Supervision of Experiments on Animals.
Acknowledgements: The authors are thankful to UGC, New Delhi and CSIR, New Delhi.
Conflict of interest: The authors declare no potential conflicts of interest.
Data availability: The data presented in this study are original data and available within the article.

References and Notes

1. A.R. Ravula, S. Yenugu. Pyrethroid based pesticides–chemical and biological aspects. *Crit. Rev. Toxicol.* **2021**, 51 (2), 117–140.
2. B.S. Rathi, P.S. Kumar, D.-V.N. Vo. Critical review on hazardous pollutants in water environment: Occurrence, monitoring, fate, removal technologies and risk assessment. *Sci. Total Environ.* **2021**, 797, 149134.
3. F. Latif, S. Aziz, R. Iqbal, et al. Impact of Pesticide Application on Aquatic Environments and Biodiversity. In *Xenobiotics in Aquatic Animals: Reproductive and Developmental Impacts*; Springer, **2023**; pp 143–164.
4. N. Khan, G. Yaqub, T. Hafeez, M. Tariq. Assessment of Health Risk due to Pesticide Residues in Fruits, Vegetables, Soil, and Water. *J. Chem.* **2020**, 2020, e5497952.
5. S.H.E. Salem, S. Abd-El Fatah, G.N.-E. Abdel-Rahman, a.S.M. Fouzy, D. Marrez. Screening for pesticide residues in soil and crop samples in Egypt. *Egypt. J. Chem.* **2021**, 64 (5), 2525–2532.
6. J. Min, J. Han, K. Kim, et al. Human cholestatic hepatitis owing to polyoxyethylene nonylphenol ingestion: A case report. *Medicine (Baltimore)* **2017**, 96 (32).
7. P.D. Virutkar, A.P. Mahajan, B.H. Meshram, S.B. Kondawar. Conductive polymer nanocomposite enzyme immobilized biosensor for pesticide detection. *J. Mater. Nanosci.* **2019**, 6 (1), 7–12..
8. H.A. Craddock, D. Huang, P.C. Turner, L. Quirós-Alcalá, D.C. Payne-Sturges. Trends in neonicotinoid pesticide residues in food and water in the United States, 1999–2015. *Environ. Health* **2019**, 18 (1), 1–16.
9. A. Marın, J.M. Vidal, F.E. Gonzalez, et al. Assessment of potential (inhalation and dermal) and actual exposure to acetamiprid by greenhouse applicators using liquid chromatography–tandem mass spectrometry. *J. Chromatogr. B* **2004**, 804 (2), 269–275.

10. O. Yeter, A. Aydın. Determination of Acetamiprid and IM-1-2 in PostMortem Human Blood, Liver, Stomach Contents by HPLC-DAD. *J. Forensic Sci.* **2014**, 59 (1), 287–292.
11. G. Ichikawa, R. Kuribayashi, Y. Ikenaka, et al. LC-ESI/MS/MS analysis of neonicotinoids in urine of very low birth weight infants at birth. *PloS One* **2019**, 14 (7), e0219208.
12. J. Ueyama, A. Aoi, Y. Ueda, et al. Biomonitoring method for neonicotinoid insecticides in urine of non-toilet-trained children using LC-MS/MS. *Food Addit. Contam. Part A* **2020**, 37 (2), 304–315.
13. A. Phogat, J. Singh, V. Malik, V. Kumar. Neuroprotective potential of berberine against acetamiprid induced toxicity in rats: Implication of oxidative stress, mitochondrial alterations, and structural changes in brain regions. *J. Biochem. Mol. Toxicol.* **2023**, e23434.
14. J. Singh, A. Phogat, C. Prakash, et al. N-Acetylcysteine Reverses Monocrotophos Exposure-Induced Hepatic Oxidative Damage via Mitigating Apoptosis, Inflammation and Structural Changes in Rats. *Antioxid. Basel Switz.* **2021**, 11 (1), 90.
15. A. Phogat, J. Singh, V. Kumar, V. Malik. Berberine mitigates acetamiprid-induced hepatotoxicity and inflammation via regulating endogenous antioxidants and NF-κB/TNF-α signaling in rats. *Environ. Sci. Pollut. Res.* **2023**, 1–12.
16. A. Ahmad, P. Kumari, M. Ahmad. Apigenin attenuates edifenphos-induced toxicity by modulating ROS-mediated oxidative stress, mitochondrial dysfunction and caspase signal pathway in rat liver and kidney. *Pestic. Biochem. Physiol.* **2019**, 159, 163–172.
17. M.S. Othman, M.A. Fareid, R.S. Abdel Hameed, A.E. Abdel Moneim. The Protective Effects of Melatonin on Aluminum-Induced Hepatotoxicity and Nephrotoxicity in Rats. *Oxid. Med. Cell. Longev.* **2020**, 2020, e7375136.
18. S. Küçükler, S. Çomaklı, S. Özdemir, C. Çağlayan, F.M. Kandemir. Hesperidin protects against the chlorpyrifos-induced chronic hepato-renal toxicity in rats associated with oxidative stress, inflammation, apoptosis, autophagy, and up-regulation of PARP-1/VEGF. *Environ. Toxicol.* **2021**, 36 (8), 1600–1617.
19. S. Devi, J. Singh, V. Kumar, V. Malik. Monocrotophos induced Biochemical and Histopathological alterations in the Kidney tissues of Mice. *Chem. Biol. Lett.* **2019**, 6 (2), 39–45.
20. B.R. Kistinger, D. Hardej. The ethylene bisdithiocarbamate fungicides mancozeb and nabam alter essential metal levels in liver and kidney and glutathione enzyme activity in liver of Sprague-Dawley rats. *Environ. Toxicol. Pharmacol.* **2022**, 92, 103849.
21. C. Gur, F.M. Kandemir. Molecular and biochemical investigation of the protective effects of rutin against liver and kidney toxicity caused by malathion administration in a rat model. *Environ. Toxicol.* **2023**, 38 (3), 555–565.
22. M. Shamsi, M. Soodi, S. Shahbazi, A. Omidi. Effect of Acetamiprid on spatial memory and hippocampal glutamatergic system. *Environ. Sci. Pollut. Res. Int.* **2021**.
23. S. Chakroun, L. Ezzi, I. Grissa, et al. Hematological, biochemical, and toxicopathic effects of subchronic acetamiprid toxicity in Wistar rats. *Environ. Sci. Pollut. Res.* **2016**, 23 (24), 25191–25199.
24. C. Prakash, V.K. Kamboj, P. Ahlawat, V. Kumar. Structural and molecular alterations in arsenic-induced hepatic oxidative stress in rats: a FTIR study. *Toxicol. Environ. Chem.* **2015**, 97 (10), 1408–1421.
25. R.L. Levine, D. Garland, C.N. Oliver, et al. Determination of carbonyl content in oxidatively modified proteins. *Methods Enzymol.* **1990**, 186, 464–478.
26. L.H. Johansson, L.H. Borg. A spectrophotometric method for determination of catalase activity in small tissue samples. *Anal. Biochem.* **1988**, 174 (1), 331–336.
27. L.A. MacMillan-Crow, J.P. Crow, J.D. Kerby, J.S. Beckman, J.A. Thompson. Nitration and inactivation of manganese superoxide dismutase in chronic rejection of human renal allografts. *Proc. Natl. Acad. Sci.* **1996**, 93 (21), 11853–11858.
28. O.H. Lowry, N.J. Rosebrough, A.L. Farr, R.J. Randall. Protein measurement with the Folin phenol reagent. *J. Biol. Chem.* **1951**, 193 (1), 265–275.
29. E.Y. Arıcan, D. Gökçeoğlu Kayalı, B. Ulus Karaca, et al. Reproductive effects of subchronic exposure to acetamiprid in male rats. *Sci. Rep.* **2020**, 10 (1), 8985.
30. B.U. Karaca, Y.E. Arican, T. Boran, et al. Toxic effects of subchronic oral acetamiprid exposure in rats. *Toxicol. Ind. Health* **2019**, 35 (11–12), 679–687.
31. R.S. Devan, A. Mishra, P.C. Prabu, T.K. Mandal, S. Panchapakesan. Sub-chronic oral toxicity of acetamiprid in Wistar rats. *Toxicol. Environ. Chem.* **2015**, 97 (9), 1236–1252.
32. J. Zhang, W. Yi, H. Xiang, et al. Oxidative stress: role in acetamiprid-induced impairment of the male mice reproductive system. *Agric. Sci. China* **2011**, 10 (5), 786–796.
33. M.E. Erdemli, E. Zayman, Z. Erdemli, et al. Protective effects of melatonin and vitamin E in acetamiprid-induced nephrotoxicity. *Environ. Sci. Pollut. Res.* **2020**, 27 (9), 9202–9213.
34. S. Yan, Z. Meng, S. Tian, et al. Neonicotinoid insecticides exposure cause amino acid metabolism disorders, lipid accumulation and oxidative stress in ICR mice. *Chemosphere* **2020**, 246, 125661.
35. M.L. Barbosa, A.-A.P.M. de Meneses, R.P.S. de Aguiar, et al. Oxidative stress, antioxidant defense and depressive disorders: A systematic review of biochemical and molecular markers. *Neurol. Psychiatry Brain Res.* **2020**, 36, 65–72.
36. A. Adwas, A. Elsayed, A. Azab, F. Quwaydir. Oxidative stress and antioxidant mechanisms in human body. *J. Biotechnol.* **2019**, 6, 43–47.
37. A.M. Pisoschi, A. Pop. The role of antioxidants in the chemistry of oxidative stress: A review. *Eur. J. Med. Chem.* **2015**, 97, 55–74.
38. N. Khovarnagh, B. Seyedalipour. Antioxidant, histopathological and biochemical outcomes of short-term exposure to acetamiprid in liver and brain of rat: The protective role of N-acetylcysteine and S-methylcysteine. *Saudi Pharm. J.* **2021**, 29(3), 280-289.
39. M.I. Shahin. Hepatoprotective effect of ginseng, green tea, cinnamon their combination against acetamiprid-induced oxidative stress in rats. *Asian J. Biol.* **2018**, 1–13.
40. S. Doltade, M. Lonare, S. Raut, A. Telang. Evaluation of Acetamiprid Mediated Oxidative Stress and Pathological Changes in Male Rats: Ameliorative Effect of Curcumin. *Proc. Natl. Acad. Sci. India Sect. B Biol. Sci.* **2019**, 89 (1), 191–199.
41. S. Gasmi, S. Chafaa, Z. Lakroun, et al. Neuronal apoptosis and imbalance of neurotransmitters induced by acetamiprid in rats. *Toxicol. Environ. Health Sci.* **2019**, 11 (4), 305–311.
42. E. Öztaş, M. Kara, T. Boran, et al. Cellular stress pathways are linked to acetamiprid-induced apoptosis in SH-SY5Y neural cells. *Biology* **2021**, 10 (9), 820.
43. B.M. Razavi, H. Hosseinzadeh, A.R. Movassaghi, M. Imenshahidi, K. Abnous. Protective effect of crocin on diazinon induced cardiotoxicity in rats in subchronic exposure. *Chem. Biol. Interact.* **2013**, 203 (3), 547–555.
44. J. Singh, A. Phogat, V. Kumar, V. Malik. N-Acetylcysteine Mediated Regulation of MnSOD, UCP-2 and Cytochrome C Associated with Amelioration of Monocrotophos-Induced Hepatotoxicity in Rats. *Toxicol. Int.* **2023**, 515–525.
45. R. Toghan, Y.A. Amin, R.A. Ali, et al. Protective effects of Folic acid against reproductive, hematological, hepatic, and renal toxicity induced by Acetamiprid in male Albino rats. *Toxicology* **2022**, 469, 153115.
46. V. Malik, J. Singh, A. Kumar, V. Kumar. Protective effect of coenzyme Q10 nanoparticles against monocrotophos induced oxidative stress in kidney tissues of rats. *Biologia (Bratisl.)* **2021**, 76, 1849-57.
47. M.H.A. Kotob, A. Hussein, M. Abd-Elkareem. Histopathological changes of kidney tissue during aging. *SVU-Int. J. Vet. Sci.* **2021**, 4 (1), 54–65.